Supplement of Earth Surf. Dynam., 8, 619–635, 2020
https://doi.org/10.5194/esurf-8-619-2020-supplement
© Author(s) 2020. This work is distributed under
the Creative Commons Attribution 4.0 License.

Supplement of

Modelling impacts of spatially variable erosion drivers on suspended sediment dynamics

Giulia Battista et al.

Correspondence to: Giulia Battista (battista@ifu.baug.ethz.ch)

The copyright of individual parts of the supplement might differ from the CC BY 4.0 License.

1 Model inputs and calibration

1.1 Soil erodibility and land cover-management factors

Figure S1 shows the spatial distribution of the soil erodibility factor K and land cover-management factor C of the Universal Soil Loss Equation for the Kleine Emme river basin. The two factors were used to derive the spatial distribution of the surface erodibility parameter α of the model. The soil erodibility factor K was taken from the work of Schmidt et al. (2018) and the land cover-management factor was derived from Yang et al. (2003).

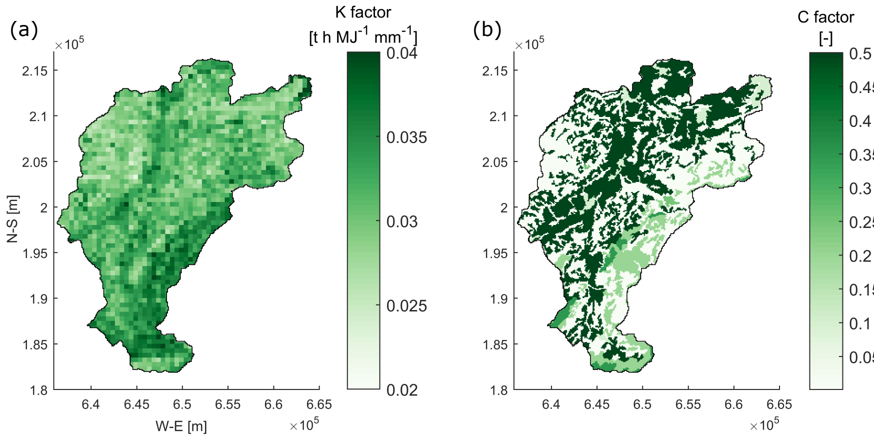

Figure S1. Maps of the (a) soil erodibility USLE factor K (source: Schmidt et al. (2018)) and (b) cover-management factor C for the Kleine Emme basin (derived from Yang et al. (2003)).

1.2 Evaluation of sediment module performance

In this section some additional metrics that evaluate the performance of the sediment model component are presented.

In Figure S2 the histogram of the simulated SSCs sampled at the hours of collection of suspended sediment bottle samples is compared with the histogram of measured SSCs smaller than the 85th percentile. The comparison of the two histograms provides an evaluation of the model performance in terms of SSC distributions.

To allow the comparison between the continuous time series of simulated hourly SSC and the intermittent observed SSC (twice a week), a continuous hourly time series has been extrapolated from the observations, based on the fitting of a Q-SSC rating curve. The comparison of observed and simulated SSCs is shown in Figure S3. In Table S1 the time series of hourly simulated and extrapolated observed SSCs are compared by means of the correlation coefficient r, percent bias PBIAS, normalized root mean square error nRMSE and mean absolute error MAE. Coherently with the approach applied in the calibration procedure (see Sect. 2.3.3 of the main text), we have limited this comparison to the observed SSC values lower than the 85th percentile of their distribution. As expected, the comparison shows a tendency to underestimate the observations and a lower performance at the hourly scale, which, however, improves with increasing temporal aggregation.

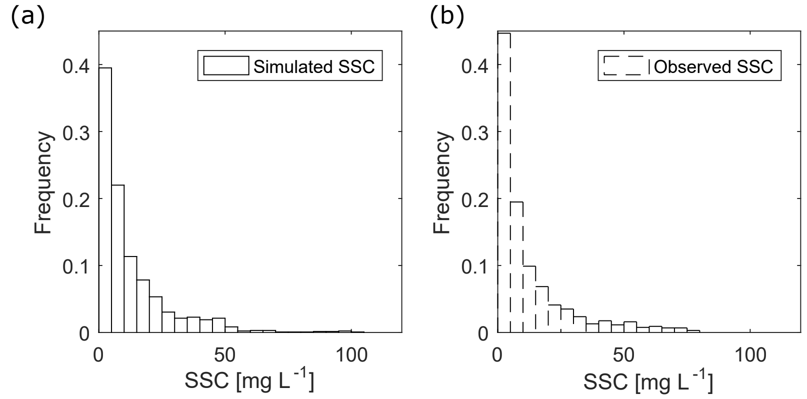

Figure S2. Simulated and observed SSC frequency distributions: (a) frequency distribution of simulated SSCs at the hours of suspended sediment sample collection, (b) frequency distribution of observed SSCs smaller than the 85th percentile.

Table S1. Performance of the suspended sediment simulations for the period 2004-2016 at the outlet of the river basin, in terms of correlation coefficient (r), Percent Bias (PBIAS), normalized root mean square error (nRMSE) and mean absolute error (MAE) for data simulated at the hourly resolution and aggregated to daily, monthly and annual values. The analyses has been limited to the values lower than the 85th percentile of the observations.

	r [-]	PBIAS [%]	nRMSE [-]	MAE [mg L^{-1}]
Hour	0.51	-12.14	1.02	8.86
Day	0.52	-12.14	0.91	9.18
Month	0.64	-12.14	0.52	5.64
Year	0.52	-12.14	0.19	2.28

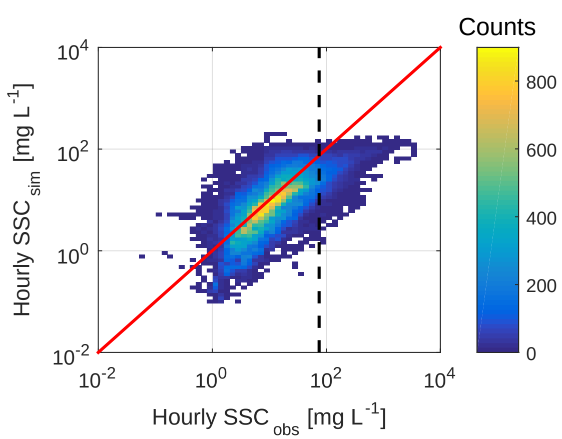

Figure S3. Density plot of simulated vs observed hourly suspended sediment concentrations at the outlet of the river basin for the period 2004-2016. The black dashed line indicates the 85th percentile of the observations, to which the performance assessment has been limited. The red line gives the 1:1 fit.

1.3 River initiation threshold effect on the hydrological model

Table S2 shows the influence of the river initiation threshold on the hydrological performance of the model. The performance is evaluated through the correlation coefficient (r), Nash-Sutcliffe efficiency (NSE) and root mean square error (RMSE). The conclusion we draw from this is that RT is not significantly influencing discharge predictions at the outlet.

Table S2. River initiation threshold (RT) effect on hydrological model performance. Observed hourly discharge data at the outlet for the period 2004-2016 are compared with two simulations with different RT values. The model performance is evaluated by means of the correlation coefficient (r), Nash-Sutcliffe efficiency (NSE) and root mean square error (RMSE) at the hourly resolution and at the daily and monthly temporal aggregation.

	r [-]		NSE [-]		RMSE [m^3 s^{-1}]	
	RT=1.25 km^2	RT=0.4 km^2	RT=1.25 km^2	RT=0.4 km^2	RT=1.25 km^2	RT=0.4 km^2
Hour	0.84	0.84	0.69	0.69	0.75	0.75
Day	0.91	0.90	0.80	0.79	0.53	0.55
Month	0.93	0.93	0.76	0.77	0.26	0.27

1.4 Hydrological model performance under dry and wet conditions

In Table S3 and Figure S4 the performance of the hydrological component of the model in reproducing events with low and high initial soil moisture (SM_0) is evaluated. These conditions have been defined as SM_0 smaller than the 20^{th} percentile of the SM_0 distribution, and SM_0 greater than the 80^{th} percentile. SM_0 is computed as the basin averaged soil moisture distribution at the last hour before the start of each event. The model performance for the selected events is good and comparable to the entire simulation, however Figure S4 indicates a tendency to overestimation especially for low SM_0 events.

Table S3. Performance of the hydrological model in reproducing low and high initial soil moisture (SM_0) events. Simulated and observed hourly discharge data at the outlet are compared for the selected events in terms of the correlation coefficient (r), Nash-Sutcliffe efficiency (NSE) and root mean square error (RMSE).

	low SM_0	high SM_0
r [-]	0.86	0.82
NSE [-]	0.74	0.63
RMSE [m^3 s^{-1}]	0.71	0.66

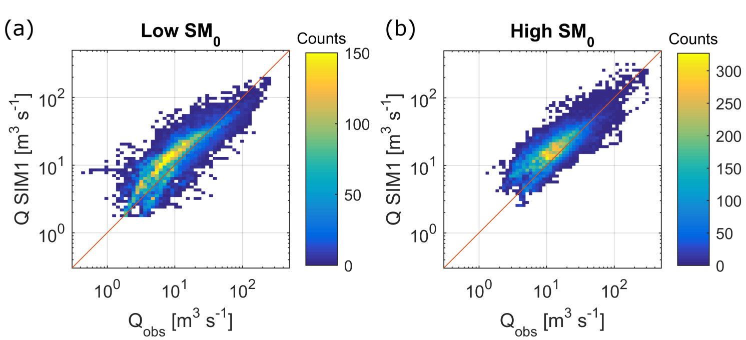

Figure S4. Density plot of simulated vs observed hourly discharges at the outlet for (a) low and (b) high initial soil moisture events within the 2004-2016 period.

2 Suspended sediment concentration variability at the outlet

The variability of suspended sediment concentration at the outlet in the four simulations is compared by means of the SSC-Q cloud of points and a coefficient of variation that quantifies their scatter. Figure S5 compares the modelled SSC (density plots) in SIMs 1 to 4 with the observations (lines). The comparison of SIM 1 and 3 with SIM 2 and 4 shows the effect of the spatial distribution of precipitation in stretching the bulk of the modelled concentrations towards higher values, which reflects the increase in the annual sediment load. Analogously, the effect of the spatial distribution of surface erodibility is opposite (compare SIM 1 and 2 with SIM 3 and 4). The plots are in log-log scale, so we point out that the differences between the simulations are more relevant at high concentrations.

To quantify the scatter of the SSC-Q relations independently of the mean simulated SSC, we binned the simulated discharges, computed the coefficients of variation (CVs) of the sediment concentrations in each discharge bin and reported them as a boxplot for all discharges in Figure S6. We observe that the distribution of the CVs shifts to lower values every time a source of variability (rainfall or α distribution) is removed, therefore, we observe a general correspondence between information content of the inputs and scatter of the predictions of SSC. However, we also observe that the changes between simulations are very small, especially in the mean value, thus suggesting that the spatially distributed nature of the model itself plays a more relevant role than the variability of the analysed input variables (rainfall and surface erodibility). The comparison of observed and simulated CVs shows the amount of variability of the lower 85th percentile of observed SSCs that is captured by the model. As expected, the observed variability is much larger than the simulated one, because of the sources of variability which are not accounted for in our model.

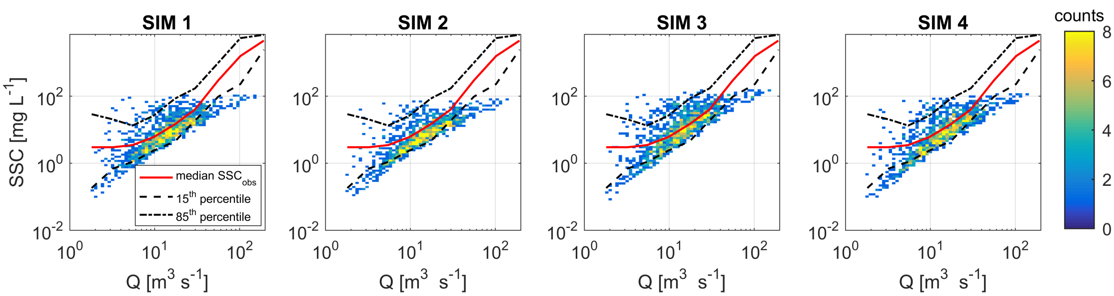

Figure S5. Density plot of simulated SSC-Q values for SIM 1 to SIM 4 sampled at the time of observations, compared with observations (lines give median and 15th-85th percentiles).

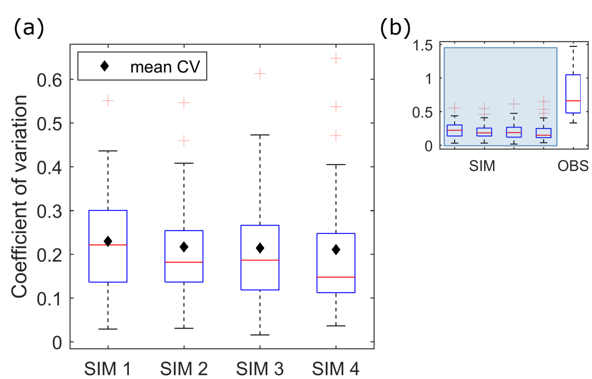

Figure S6. Quantification of the SSC-Q relation scatter: (a) boxplots of the coefficients of variation of the SSC-Q relation for SIM 1 to SIM 4, (b) comparison of simulated (blue box) and observed coefficients of variations, where the observed SSCs have been truncated to the 85th percentile.

References

Schmidt, S., Ballabio, C., Alewell, C., Panagos, P., and Meusburger, K.: Filling the European blank spot—Swiss soil erodibility assessment with topsoil samples, Journal of Plant Nutrition and Soil Science, 181, 737–748, https://doi.org/10.1002/jpln.201800128, 2018.

Yang, D., Kanae, S., Oki, T., Koike, T., and Musiake, K.: Global potential soil erosion with reference to land use and climate changes, Hydrological Processes, 17, 2913–2928, https://doi.org/10.1002/hyp.1441, 2003.